J. Phys. Chem. A **2004,** *108,* 2930−2935

Proton Affinity of Peroxyacetic Acid[†]

Charles E. Miller*[,‡]

Department of Chemistry, Haverford College, Haverford, Pennsylvania 19041-1392

Joseph S. Francisco[§]

Department of Chemistry and Department of Earth and Atmospheric Science, Purdue University, West Lafayette, Indiana 47907-1393

Received: September 15, 2003; In Final Form: January 2, 2004

The proton affinity of peroxyacetic acid has been studied using ab initio methods. The most stable peroxyacetic acid structure forms a nearly planar five-membered ring in which the carbonyl oxygen atom is hydrogen bonded to the acidic hydrogen atom. The rotational constants, dipole moments, and harmonic vibrational frequencies obtained for this structure are in excellent agreement with available experimental data. Calculations on the protonated peroxyacetic acid system identified low energy structures associated with protonation at each of the three chemically distinguishable oxygen atom sites. Protonation at the carbonyl oxygen site leads to the lowest energy protomer with an optimized structure that also contains a five-membered ring formed by intramolecular hydrogen bonding. The relative energies and proton affinities have been determined at the QCISD and QCISD(T) levels of theory. Additional calculations performed with the ab initio model chemistries CBS-4, CBS-Q, CBS-APNO, and G2(MP2) are in good agreement with the QCISD(T)/6-311+G(2df,2p) proton affinity. The CBS-Q prediction for the proton affinity of peroxyacetic acid, $\mathrm{PA}^{0\mathrm{K}}_{\mathrm{CBS-Q}} = -775.9$ kJ mol^{-1}, differs by only 2.5 kJ mol^{-1} from the proton affinity recently calculated for peroxyacetyl nitrate, $\mathrm{PA}^{0\mathrm{K}}_{\mathrm{CBS-Q}} = -773.4$ kJ mol^{-1}, and outside the error limits of the experimental measurement attributed to the proton affinity of peroxyacetyl nitrate, -798 ± 12 kJ mol^{-1}.

Introduction

We recently reported ab initio calculations which predicted that the most stable protomer of peroxyacetyl nitrate (PAN) is a peroxyacetic acid−nitronium ion complex [$CH_3C(O)OOH\cdots NO_2^+$], consistent with the most stable structures of other protonated nitrates.[1] That study demonstrated that an accurate determination of the proton affinity of PAN will be difficult since several alternate low energy PAN protomers were also identified. The [$CH_3C(O)OOH\cdots NO_2^+$] complex will also act as a facile nitrating agent, further complicating experimental measurements. Additionally, Hansel and Wisthalter[2] observed rapid formation of protonated peroxyacetic acid when protonated PAN was created in the presence of trace amounts of water vapor

$$[CH_3C(O)OOH\cdots NO_2^{\ +}] + H_2O \rightarrow CH_3C(O)OOH_2^{\ +} + HNO_3 \quad (R1)$$

Srinivasan et al.[3] used a bracketing/collision induced dissociation technique with mass spectroscopic detection to measure a proton affinity of $\mathrm{PA}^{298\mathrm{K}}$ (PAN) $= -798 \pm 12$ kJ mol^{-1} that they attributed to protonation of the carbonyl oxygen atom. In reference 1, we argued that the experimental proton affinity and the assumed structure of protonated PAN were inconsistent with the chemical characteristics of PAN. However, rapid reaction of the [$CH_3C(O)OOH\cdots NO_2^+$] complex with the adduct gases present in the Srinivasan et al. experiments could produce significant quantities of protonated peroxyacetic acid via mechanisms analogous to R1

$$[CH_3C(O)OOH\cdots NO_2^{\ +}] + HX \rightarrow CH_3C(O)OOH_2^{\ +} + XNO_2 \quad (R2)$$

Protonation of peroxyacetic acid at the carbonyl oxygen position would be expected and would agree with the protonation mechanism Srinivasan et al. proposed to interpret their results. The proton affinity of peroxyacetic acid is unknown, but is expected to be 20−40 kJ mol^{-1} larger than the proton affinity of PAN,[1] $\mathrm{PA}^{0\mathrm{K}}_{\mathrm{CBS-Q}}(\mathrm{PAN}) = -773.4 \pm 10$ kJ mol^{-1}, based on the proton affinities of other carboxylic acids and their nitrate derivatives.[4]

There exists very limited experimental or theoretical information concerning the structure and physical properties of peroxyacetic acid. Cugley et al. observed the rotational spectrum of gas-phase peroxyacetic acid from which they obtained rotational constants, dipole moments, and an estimated molecular structure.[5] In a separate work, Cugley, Meyer, and Gunthard isolated peroxyacetic acid and several of its deuterated isotopomers in low-temperature Ar matrixes and recorded their infrared spectra.[6] The vibrational frequencies and normal coordinate analysis from this work were consistent with intramolecular hydrogen bonding between the carbonyl oxygen atom and the acidic hydrogen atom, estimated as 20−30 kJ mol^{-1} from the torsional transitions observed in the microwave

---

[†] Part of the special issue “Fritz Schaefer Festschrift”.

[*] Corresponding author.

[‡] Present address: Jet Propulsion Laboratory, California Institute of Technology, MS 183-501, 4800 Oak Grove Drive, Pasadena, CA 91109-8099. E-mail: charles.e.miller@jpl.nasa.gov.

[§] E-mail: jfrancis@chem.purdue.edu.

10.1021/jp036748w CCC: $27.50

TABLE 1: Optimized Peroxyacetic Acid Structures

parameter	descrption	B3LYP/ 6-311+G(3df,3pd)	MP2/ 6-311+G(2d,2p)	QCISD/ 6-311+G(2d,2p)	ref 7 MP2(full)/6-31G*	ref 5 experimental model
Bond Lengths (Å)						
R(1,2)	C−C	1.498	1.494	1.502	1.497	1.49
R(1,6)	C−H	1.089	1.084	1.087	1.092	1.09
R(1,7)	C−H	1.089	1.082	1.087	1.092	1.09
R(1,8)	C−H	1.086	1.084	1.085	1.089	1.09
R(2,3)	C−O	1.350	1.355	1.353	1.359	1.33
R(2,5)	C═O	1.206	1.212	1.208	1.220	1.22
R(3,4)	O−O	1.433	1.443	1.437	1.457	1.47
R(4,9)	O−H	0.983	0.980	0.975	0.993	1.00
R(5,9)	C═O···HO	1.871	1.853	1.873	1.865	1.82
Bond Angles (degrees)						
A(2,1,6)		108.6	108.5	108.5	108.7	108.8
A(2,1,7)		108.6	108.5	108.5	108.7	108.8
A(2,1,8)	<CCH	111.9	111.6	111.5	111.4	108.8
A(6,1,7)		107.9		108.4		
A(6,1,8)		109.9		110.0		
A(7,1,8)		109.9		110.0		
A(1,2,3)	<CCO	111.2	110.6	111.1	110.5	110.0
A(1,2,5)	<CC═O	126.9	127.1	126.7	127.0	130.0
A(3,2,5)	<OC═O	121.9	122.2	122.2		120.0
A(2,3,4)		111.4		110.9		
A(3,4,9)	<OOH	100.6	100.0	100.7	99.7	96.6
Energy (hartrees)						
		−304.33577	−303.72068	−303.63501		

spectrum.[5] The only previous theoretical work on peroxyacetic acid reported an optimized MP2/6-31G* structure similar to that inferred from the microwave spectrum and used the CBS-Q model chemistry to estimate a value of 48 kcal mol^{-1} for the O−O bond.[7] Colussi and Grela estimated a similar O−O bond dissociation energy from bond contribution arguments.[8]

This paper continues our ab initio studies of the chemical and physical properties of PAN and related molecules.[1,9−11] Here we present a systematic investigation of the structure, harmonic force field, and proton affinity of peroxyacetic acid with the goal of better understanding experimental attempts to measure the proton affinity of PAN.[2,3]

Computational Methods and Results

The computational methods employed in this study are similar to those employed previously in our studies of peroxyacetyl nitrate[1,9] and acetic acid.[11] All calculations were performed using the GAUSSIAN 98 program suite.[12] Optimized molecular structures were computed with the Becke3−Lee−Yang−Parr (B3LYP) density functional,[13] Møller−Plesset perturbation theory with second-order corrections (MP2),[14−18] quadratic configuration interaction with single and double excitations (QCISD) using the basis sets 6-31G* through 6-311++G(3df,3pd).[19−23] Single-point energy calculations were also performed using QCISD with a partial treatment of triple excitations (QCISD(T)).[24] Thermochemical calculations employed the complete basis set (CBS) model chemistries CBS-4, CBS-Q, and CBS-APNO[25] as well as the G2(MP2) method.[26] Our previous work showed that the CBS-Q method yields bond energies and proton affinities with ±10 kJ mol^{-1} accuracy for PAN-type molecules and radicals.[1,9] The CBS-APNO method may be expected to yield results with ±2 kJ mol^{-1} accuracy.[25]

Results and Discussion

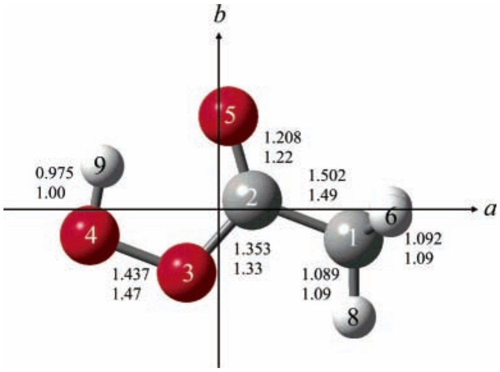

Figure 1. Peroxyacetic acid structure. The bond lengths (in angstroms) are from the optimized QCISD/6-311+G(2d,2p) calculations (top), the experimental model structure inferred from microwave spectroscopy by Cugley et al.[5] (bottom). The *a* and *b* components of the principal axis system are also shown.

1. Peroxyacetic Acid. *Structure*. Survey calculations performed at the QCISD/6-31G(d) level of theory revealed the presence of multiple conformational minima on the peroxyacetic acid potential surface. The lowest energy structure possesses a nearly planar five-membered ring with the carbonyl O atom (O_5) hydrogen bonded to the acidic H atom (H_9), as shown in Figure 1. Full structural optimizations were performed at the B3LYP/6-311+G(3df,3pd), MP2/6-311+G(2d,2p), and QCISD/6-311+G(2d,2p). The results are reported in Table 1 along with the MP2/6-31G* structure calculated by Bach, Ayala and Schlegel.[7] The theoretical r_e structures are also compared to the r_0 structure inferred by Cugley et al. from the microwave spectrum of gas-phase peroxyacetic acid.[5] The QCISD/6-311+G(2d,2p) r_e structure is considered the most accurate, although calculations at all levels of theory produced similar results.

There is good agreement between the optimized QCISD/6-311+G(2d,2p) structure and the structure estimated from the microwave spectrum; however, there are differences that merit attention. The largest difference is in the intramolecular hydrogen bond where the ab initio structure predicts a C═O···H−O bond length of 1.873 Å, 0.053 Å longer than the 1.82 Å hydrogen bond length inferred from the Cugley et al. model structure.[5] Both bond lengths are consistent with strong internal hydrogen bonding, 25−30 kJ mol^{-1} according to the O−H vibrational frequency shift observed in the infrared spectrum[6]

TABLE 2: Peroxyacetic Acid Rotational Constants (MHz)

rotational constant	B3LYP/ 6-311+G(3df,3pd)	MP2/ 6-311+G(2d,2p)	QCISD/ 6-311+G(2d,2p)	Cugley et al. ref 5
A	10896	10788	10849	10815
B	4274	4293	4270	4275
C	3129	3130	3123	3122

TABLE 3: Rotational Constants (MHz) for Deuterated Peroxyacetic Acid Isotopologues Calculated at the B3LYP/6-311+G(3df,3pd) Level of Theory

rotational constant	$CH_3C(O)OOD$ ref 5	$CH_3C(O)OOD$	$CD_3C(O)OOH$	$CD_3C(O)OOD$
A	10686	10753	10014	9906
B	4193	4191	3776	3701
C	3068	3073	2838	2787

TABLE 4: Peroxyacetic Acid Dipole Moments (Debeye)

dipole component	MP2/ 6-311+G(2d,2p)	B3LYP/ 6-311+G(3df,3pd)	QCISD/ 6-311+G(2d,2p)	ref 5 preferred	ref 5 alternate
μ_a	2.5574	2.3361	2.5058	2.294(3)	2.304(3)
μ_b	−0.6400	−0.5991	−0.6334	0.650(4)	−0.614(4)
μ_c	0.0007	0.0009	0.0003	0.000[a]	0.000[a]
μ_{TOTAL}	2.6363	2.4117	2.5846	2.384(5)	2.384(5)

[a] Fixed.

(see below). Some of the discrepancy may also be absorbed by small changes in other structural parameters associated with the five-membered ring. For instance, the ab initio value of the O−O bond length is 1.437 Å, 0.033 Å smaller than the 1.47 Å value assumed for the experimental structure. Likewise, the ab initio calculations predict a O−H bond length of 0.975 Å, 0.025 Å shorter than the experimental model value of 1.00 Å. Simultaneously, the ab initio structure predicts a more open ∠OOH, 100.7° vs 96.6° from the experimental model structure. Finally, Cugley et al. note that if their measured nonzero value for the μ_c dipole component is real, it would result in a dihedral angle of 10° about the O−O bond.[5] However, the ab initio structure predicts a planar peroxy acid group and this is supported by the known change of the inertial defect measured upon deuteration.[5]

The experimental and ab initio structures show better agreement for the bonding about the two carbon centers. There is no significant difference between the descriptions of the CH_3 group, although it was discovered that the QCISD calculations required a O═C−C−H dihedral angle deviating slightly from 180° to produce a complete set of real vibrational frequencies, i.e., find the true minimum on the potential. Bach, Ayala and Schlegel reported the same CH_3 group orientation in their optimized peroxyacetic acid structure.[7] The bonding around the carbonyl carbon exhibits classic sp^2 character with very small differences between the ab initio and experimental C═O (1.208 Å vs 1.22 Å), C−O (1.353 Å vs 1.33 Å), and C−C (1.502 Å vs 1.49 Å) bond lengths. The ab initio structure predicts a contracted ∠CC═O compared to the experimental model, (126.7° vs 130.0°) with a corresponding opening of ∠OCO (122.2° vs 120.0°) and ∠CC−O (111.1° vs 110.0°).

The quality of the ab initio structures is supported by the excellent agreement between the theoretical and experimental[5] rotational constants. Table 2 shows that the QCISD/6-311+G(2d,2p) rotational constants reproduce the experimental *B* and *C* constants for $CH_3C(O)OOH$ almost perfectly. The 34 MHz overestimate of the *A* constant is still an excellent result, representing only a 0.3% deviation. The B3LYP/6-311+G(3df,3pd) and MP2/6-311+G(2d,2p) rotational constants also reproduce the experimental values.

We have also calculated rotational constants for the $CH_3C(O)OOD$, $CD_3C(O)OOH$, and $CD_3C(O)OOD$ isotopologues at the B3LYP/6-311+G(3df,3pd) level of theory. These results are collected in Table 3. The agreement between the experimental and B3LYP rotational constants for $CH_3C(O)OOD$ is again excellent, although the discrepancy in the *A* constant persists. Examining the trend in the *A* rotational constant as a function of deuteration, it appears that this parameter is largely determined by the hydrogen atoms of the methyl group. Discrepancies in the theoretical values for *A* therefore seem likely due to small inaccuracies in the positions of the methyl hydrogens.

Further evidence of the accuracy of the ab initio structures comes from a comparison of the theoretical and experimental dipole moments. Table 4 lists values of the dipole moment components in the principal axis system along with the preferred and alternate dipole moment solutions reported by Cugley et al.[5] The theoretical calculations unambiguously favor a negative μ_b which matches with the alternate solution determined by Cugley et al. The preference for the positive μ_b solution in the experimental study was based on an estimate from bond moments: $\mu_a = 1.94$ D and $\mu_b = 0.56$ D.[5] It is unclear why the bond moment estimate yielded $\mu_b > 0$. Nevertheless, the quantitative agreement between the ab initio and experimental dipole moment components and total dipole moment provide confidence that the optimized ab initio structures have captured the salient features of the true peroxyacetic acid structure.

Vibrational Frequencies. Harmonic vibrational frequencies have been calculated at the B3LYP/6-311+G(3df,3pd) level of theory for $CH_3C(O)OOH$, $CH_3C(O)OOD$, $CD_3C(O)OOH$, and $CD_3C(O)OOD$. The calculated frequencies and intensities are presented in Tables 5−8. The experimental frequencies, intensities, and normal coordinate analysis (NCA) frequencies determined from the spectra of peroxyacetic acid samples deposited on a 4 K Ar matrix by Cugley et al.[6] have been included for comparison. As mentioned above, a gauche orientation of the methyl group was required to obtain a complete set of positive harmonic frequencies. Calculations performed using the eclipsed structure of Cugley et al.[5] resulted in one or more imaginary frequencies.

There is good overall agreement between the experimental and B3LYP frequencies for the parent and all deuterated isotopologues of peroxyacetic acid. Density functional calculations of the low frequency modes typically fall within 3% of

TABLE 5: $CH_3C(O)OOH$ Vibrational Frequencies (cm^{-1}) and Intensities (km mol^{-1})

mode	expt ref 6	NCA ref 6	B3LYP/ 6-311++G(3df,3pd)
ν_1	3282 w	3312	3491 (83.8)
ν_2	3025 w	3027	3154 (2.8)
ν_3		2902	3058 (0.3)
ν_4	1767 s	1766	1792 (226.8)
ν_5	1439 s	1443	1488 (128.8)
ν_6		1433	1478 (2.6)
ν_7	1369 m	1371	1401 (13.4)
ν_8	1234 s	1231	1252 (199.0)
ν_9	940 m	937	1029 (3.1)
ν_{10}	865 s	866	901 (42.8)
ν_{11}		810	980 (0.4)
ν_{12}	619 s	611	637 (27.3)
ν_{13}	449 w	437	432 (12.1)
ν_{14}	318 s	312	318 (16.9)
ν_{15}	3005 w	3024	3124 (0.9)
ν_{16}	1429 m	1430	1476 (8.3)
ν_{17}	1040 m	1040	1063 (9.9)
ν_{18}	646 m	647	653 (8.7)
ν_{19}	422 s	413	482 (68.6)
ν_{20}		217	227 (0.4)
ν_{21}		60	50 (0.4)

TABLE 6: $CH_3C(O)OOD$ Vibrational Frequencies (cm^{-1}) and Intensities (km mol^{-1})

mode	expt ref 6	NCA ref 6	B3LYP/ 6-311++G(3df,3pd)
ν_1		3027	3154 (2.9)
ν_2		2902	3058 (0.3)
ν_3	2433 m	2413	2542 (49.5)
ν_4	1756 m	1764	1787 (236.4)
ν_5		1433	1479 (9.3)
ν_6	1369 m	1372	1402 (9.8)
ν_7	1233 s	1232	1252 (199.9)
ν_8	1103 m	1103	1137 (38.9)
ν_9	934 m	936	1063 (8.8)
ν_{10}	854 s	852	886 (47.5)
ν_{11}		794	975 (0.1)
ν_{12}	610 m	607	627 (10.4)
ν_{13}	432 m	433	425 (10.4)
ν_{14}	311 m	302	309 (17.8)
ν_{15}		3024	3124 (0.9)
ν_{16}		1430	1476 (8.4)
ν_{17}	1043 w	1040	1023 (5.1)
ν_{18}		643	647 (7.7)
ν_{19}	320 s	331	357 (44.3)
ν_{20}		200	226 (0.8)
ν_{21}		60	50 (0.4)

TABLE 7: $CD_3C(O)OOH$ Vibrational Frequencies (cm^{-1}) and Intensities (km mol^{-1})

mode	expt. ref 6	NCA ref 6	B3LYP/ 6-311++G(3df,3pd)
ν_1	3285 m	3312	3491 (87.5)
ν_2		2264	2339 (1.4)
ν_3		2089	2197 (0.1)
ν_4	1760 s	1759	1791 (229.3)
ν_5	1442 s	1443	1486 (121.1)
ν_6	1247 vs	1249	1258 (196.1)
ν_7	1071	1066	1098 (14.8)
ν_8		1038	1063 (3.0)
ν_9	905 m	903	936 (9.2)
ν_{10}	786 m	799	916 (12.7)
ν_{11}		699	799 (14.6)
ν_{12}	551 s	550	573 (38.7)
ν_{13}	398 w	405	410 (17.7)
ν_{14}	297 m	307	298 (10.9)
ν_{15}		2256	2312 (0.4)
ν_{16}	1032 m	1031	1052 (15.2)
ν_{17}	917 m	911	955 (9.5)
ν_{18}		559	607 (7.9)
ν_{19}	416 vs	407	474 (53.3)
ν_{20}		210	216 (0.3)
ν_{21}		44	37 (0.2)

TABLE 8: $CD_3C(O)OOD$ Vibrational Frequencies (cm^{-1}) and Intensities (km mol^{-1})

mode	expt ref 6	NCA ref 6	B3LYP/ 6-311++G(3df,3pd)
ν_1	2434 m	2413	2542 (49.5)
ν_2		2264	2339 (1.5)
ν_3		2089	2197 (0.1)
ν_4	1754 s	1757	1784 (238.7)
ν_5	1247 vs	1251	1258 (206.0)
ν_6	1108 s	1105	1138 (29.9)
ν_7	1065 m	1064	1092 (18.9)
ν_8		1038	1063 (3.1)
ν_9	897 m	895	954 (8.7)
ν_{10}	783 m	775	796 (16.2)
ν_{11}		699	914 (10.0)
ν_{12}	543 m	548	556 (9.7)
ν_{13}	400 s	401	400 (15.5)
ν_{14}	293 m	297	292 (12.0)
ν_{15}		2256	2312 (0.4)
ν_{16}	1031 m	1031	1052 (15.2)
ν_{17}	903 m	911	916 (14.5)
ν_{18}		554	601 (7.6)
ν_{19}	320 vs	326	356 (42.5)
ν_{20}		191	214 (0.6)
ν_{21}		44	37 (0.2)

the matrix value. The B3LYP calculations systematically overestimate the C−H and O−H stretching frequencies by 100−200 cm^{-1}. Despite this, we note that the B3LYP O−H and O−D stretching frequencies are red-shifted 600−700 cm^{-1} as a result of the intramolecular hydrogen bonding, consistent with experiment. There are also some discrepancies in the data for modes in the 600−900 cm^{-1} range. Many of the normal modes occurring at these frequencies are heavily mixed, containing significant contributions from three or more internal coordinates. Discrepancies between the B3LYP and experimental or NCA frequencies arise from the slightly different potential energy distributions. This chiefly affects weak transitions or those unobserved in the experimental spectrum.

The B3LYP calculations for the deuterated isotopologues reproduce the position-sensitive vibrational frequency shifts very well as exemplified by a comparison of the results for $CH_3C(O)OOH$ and $CH_3C(O)OOD$. Shifts in the O−H stretch and OOH bend frequencies characterize deuteration at the terminal H atom site. As noted above, the B3LYP overestimate the O−H (O−D) stretching frequencies by 200 (100) cm^{-1} compared to the experimental Ar matrix values.[6] However, the ν_{O-D}/ν_{O-H} ratios, 0.728 for the B3LYP calculations and 0.741 for the experimental frequencies, are in good agreement. Excellent agreement is observed for the frequencies and intensities of the OOH bending mode. The B3LYP calculation reproduces the large deuteration shift of this mode, dropping from 1488 cm^{-1} to 1137 cm^{-1}. These values are 3% larger than the experimental values, but the B3LYP ν_{OOD}/ν_{OOH} ratio, 0.764, reproduces the experimental ratio, 0.767, very well.

2. Protonated Peroxyacetic Acid. *Structure*. Survey calculations identified low energy structures associated with protonation of peroxyacetic acid at the three oxygen atom sites. Calculations using the CBS-4, CBS-Q, and G2(MP2) model chemistries demonstrated that protonation at the carbonyl oxygen atom site yields the most stable structure (Table 9). A series of calculations were performed at the B3LYP/6-31G(d) level of theory to locate the minimum energy conformation with respect to the orientation of the $\angle H_{10}O_5C_2O_3$, $\angle O_5C_2O_3O_4$, and $\angle C_2O_3O_4H_9$ dihedral

TABLE 9: Model Chemistry Energies (hartrees) for Peroxyacetic Acid Protonated at Three Different Oxygen Atom Sites (see Figure 2)

protonation site	CBS-4	CBS-Q	G2(MP2)
O_5	−304.13861	−304.10783	−304.08594
O_3	−304.11658	−304.08655	−304.06536
O_4	−304.09760		

TABLE 10: Conformational Analysis of $[CH_3C(OH)OOH]^+$ Protomers at the B3LYP/6-31G(d) Level of Theory

structure	$\tau(O_4O_3C_2O_5)$ (degrees)	$\delta_1(H_9O_4O_3C_2)$ (degrees)	$\delta_4(H_{10}O_5C_2O_3)$ (degrees)	energy (hartrees)
c_1	0.0	0.0	0.0	−302.83924
c_2	0.0	180.0	0.0	−302.87661
c_3	0.0	0.0	180.0	−302.85795
c_4	0.0	180.0	180.0	−302.87072
c_5	180.0	0.0	0.0	−302.83964
c_6	180.0	180.0	0.0	−302.86660
c_7	180.0	0.0	180.0	−302.84827
c_8	180.0	180.0	180.0	−302.87128

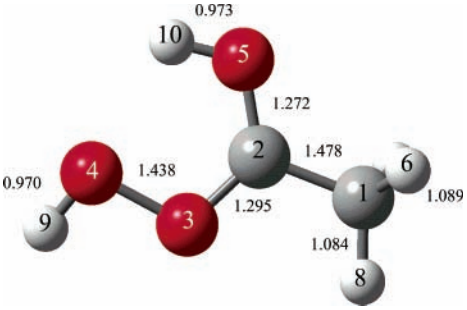

Figure 2. The optimized QCISD/6-311+G(2d,2p) structure calculated for protonated peroxyacetic acid. All bond lengths are in angstroms.

angles. The results are collected in Table 10. The minimum energy conformation is one in which the heavy atoms remain nearly planar: H_{10} forms an intramolecular hydrogen bond with O_4 and this forces the H_9 to rotate away from O_5, as shown in Figure 2. Similar intramolecular hydrogen bonding has been determined for protonated tropolone.[27] The protonated peroxyacetic acid structure was optimized at the QCISD level of theory using the 6-31G(d), 6-311+G(d,p) and the 6-311+G(2d,2p) basis sets. Single point energy calculations were performed at the QCISD(T)/6-311+G(2d,2p) and QCISD(T)/6-311+G(2df,2p) levels of theory using the optimized QCISD/6-311+G(2d,2p) structure. The energies are listed in Table 11 and the optimized bond lengths are provided in Figure 2.

Protonation induces substantial structural reorganization around the carbonyl carbon center, C_2. Compared to the neural structure, the $C_2{=}O_5$ bond elongates 0.075 Å to 1.272 Å while the $C_2{-}O_3$ bond contracts 0.080 Å to 1.295 Å, rendering the two carbon−oxygen bonds nearly equivalent. This result signals a reduction in the sp^2 character at the carbon atom and greater delocalization of the electron density over the $O_5{-}C_2{-}O_3$ linkage. The redistribution of electron density about C_2 also induces contractions of 0.025 Å and 0.012 Å in the $C_2{-}C_1$ and $O_3{-}O_4$ bonds, respectively.

The intramolecular hydrogen bond is a mirror image of the bond formed in the neutral molecule. The bond is now formed by H_{10}, the hydrogen atom attached at the former carbonyl oxygen atom, and O_4, the oxygen atom at the end of the peroxy acid group. The hydrogen bond distance has increased from 1.873 Å in the neutral to 1.999 Å in protonated peroxyacetic acid, indicating a decrease in the strength of the hydrogen bonding. We also note that, aside from the participation of H_{10} in the intramolecular hydrogen bond, there is little difference between H_9 and H_{10}. Their atomic charges are very similar, 0.350 vs 0.335, and the $O_5{-}H_{10}$ and $O_4{-}H_9$ bond lengths are nearly identical, 0.973 vs 0.970.

Examination of the other atoms shows that all of the significant charge density is located around the intramolecular ring. The carbon atom C_2 carries the largest positive charge, 0.670, while the hydrogen atoms H_{10} and H_9 carry very similar charges, 0.335 and 0.350, respectively. The negative charges on the oxygen atoms in the peroxy chain, −0.219 on O_3 and −0.132 on O_4, coupled with the −0.341 charge on O_5 leave the ring with a net positive charge of 0.66. Bouchoux and co-workers presented similar results for protonated acetic anhydride[28] and a number of phenols.[29]

Proton Affinity. The proton affinity of peroxyacetic acid has been computed at the QCISD and QCISD(T) levels of theory using several basis sets and a zero point energy correction based on QCISD/6-31G(d) harmonic frequencies for both neutral and protonated peroxyacetic acid. The results are given in Table 11. Proton affinity calculations were also performed using the CBS-4, CBS-Q, CBS-APNO, and G2(MP2) model chemistries. The results of these calculations are collected in Table 12.

The agreement between the QCISD(T)/6-311+G(2df,2p)//QCISD/6-311+G(2d,2p) and CBS-APNO proton affinities, $PA_{QCISD(T)} = -780.7$ kJ mol^{-1} and $PA^{0K}_{CBS-APNO} = -778.8$ kJ mol^{-1}, is excellent, with the difference of 1.9 kJ mol^{-1} falling within the ± 2.0 kJ mol^{-1} deviation expected for the CBS-APNO method. We note that the peroxyacetic acid proton affinity lies 5 kJ mol^{-1} below the value calculated for PAN[1], $PA(PAN)^{0K}_{CBS-Q} = -773.4$ kJ mol^{-1}. The theoretical peroxyacetic acid proton affinity also falls significantly short of the experimental measurement of −798 ± 12 kJ mol^{-1} measured by Srinivasan et al.[3] for the PAN system using collision-induced dissociation. Prior to performing proton affinity calculations for peroxyacetic acid, we hypothesized that the Srinivasan et al. experiments might have measured the proton affinity of peroxyacetic acid due to reactions R1 and R2, since the ∼20 kJ mol^{-1} discrepancy is consistent with the difference one might expect on the basis of the proton affinities of other carboxylic acids and their nitrate derivatives.[4] However, our results indicate that protonated peroxyacetic acid is only 5 kJ mol^{-1} more stable than $PANH^+$. The crucial difference in the empirical estimate

TABLE 11: $PA(CH_3C(O)OOH)$ Calculated Using the QCISD and QCISD(T) Methods

level of theory	$CH_3C(O)OOH$ (hartrees)	$[CH_3C(OH)OOH]^+$ (hartrees)	ΔZPE[a] (kJ mol^{-1})	proton affinity (kJ mol^{-1})
QCISD/6-31G(d)	−303.38171	−303.69256	30.84	−785.2
QCISD/6-311+G(d,p)	−303.56486	−303.87873	30.84	−793.1
QCISD/6-311+G(2d,2p)	−303.63501	−303.94708	30.84	−788.4
QCISD(T)/6-311+G(2d,2p)[b]	−303.67469	−303.98459	30.84	−782.7
QCISD(T)/6-311+G(2df,2p)[b]	−303.76696	−304.07613	30.84	−780.7

[a] Zero-point energies calculated at the QCISD/6−31G(d) level of theory. [b] Single-point energies calculated at the optimized QCISD/6-311+G(2d,2p) geometries.

TABLE 12: Proton Affinity of Peroxyacetic Acid (0 K)

composite method	$CH_3C(O)OOH$ (hartrees)	$[CH_3C(OH)OOH]^+$ (hartrees)	proton affinity (kJ mol^{-1})
G2(MP2)	−303.788719	−304.078600	−761.1
CBS-4	−303.843310	−304.138600	−775.3
CBS-Q	−303.812313	−304.107830	−775.9
CBS-APNO	−304.149199	−304.445827	−778.8

appears to be the peroxide linkage and the intramolecular hydrogen bonding it enables in the peracid. The potential assignment of the Srinivasan et al. measurement to PA($CH_3C(O)OOH$) becomes even less likely given that the calculated at room-temperature value, $PA_{CBS-APNO}^{295K} = -775.4$ kJ mol^{-1}, lies 3.4 kJ mol^{-1} further below the experimental number. We cannot at present reconcile the theoretical proton affinities of either PAN or peroxyacetic acid with the Srinivasan et al.[3] work and conclude that that a definitive experimental value for PA(PAN) remains to be measured.

Conclusions

The structure, harmonic vibrational frequencies and proton affinity of peroxyacetic acid have been investigated using ab initio methods. The results describe a molecule with strong intramolecular hydrogen bonding between the carbonyl oxygen atom and the hydrogen atom of the peroxy acid group. The calculated rotational constants, dipole moments, and vibrational frequencies for peroxyacetic acid and its deuterated isotopologues are in excellent agreement with the available experimental data.[5,6] Proton affinities computed using the QCISD and QCISD(T) methods as well as a number of model chemistry algorithms yielded consistent results. The most accurate proton affinity, $PA_{CBS-APNO}^{295K} = -775.4 \pm 2.0$ kJ mol^{-1}, lies 22.6 kJ mol^{-1} below the experimental the value of -798 ± 12 kJ mol^{-1} measured in the experiments of Srinivasan et al.[3] and suggests that neither protonation of peroxyacetic acid nor PAN account for their results.

Acknowledgment. The authors thank the NASA Jet Propulsion Laboratory for ample computing resources to conduct this research. The NASA Office of Space Science and Applications sponsors the Jet Propulsion Laboratory Supercomputing Project.

References and Notes

(1) Miller, C. E.; Francisco, J. S. *J. Phys. Chem. A* **2001**, *105*, 750.
(2) Hansel, A.; Wisthlaer, A. *Geophys. Rev. Lett.* **2000**.
(3) Srinivasan, N.; Cooks, R. G.; Shepson, P. B. *Rapid Commun. Mass Spectrom.* **1998**, *12*, 328.
(4) Hunter, E. P. L.; Lias, S. G. *J. Phys. Chem. Ref. Data* **1998**, *27*, 413.
(5) Cugley, J. A.; Bossert, W.; Bauder, A.; Gunthard Hs, H. *Chem. Phys.* **1976**, *16*, 229.
(6) Cugley, J.; Meyer, R.; Gunthard Hs, H. *Chem. Phys.* **1976**, *18*, 281.
(7) Bach, R. D.; Ayala, P. Y.; Schlegel, H. B. *J. Am. Chem. Soc.* **1996**, *118*, 12758.
(8) Colussi, A. J.; Grela, M. A. *Int. J. Chem. Kinet.* **1998**, *30*, 41.
(9) Miller, C. E.; Lynton, J. I.; Keevil, D. M.; Francisco, J. S. *J. Phys. Chem. A* **1999**, *103*, 11451.
(10) Miller, C. E.; Francisco, J. S. *J. Phys. Chem. A* **2000**.
(11) Miller, C. E.; Francisco, J. S. *Chem. Phys. Lett.* **2002**, *364*, 427.
(12) Frisch, M. J.; Trucks, G. W.; Schlegel, H. B.; Scuseria, G. E.; Robb, M. A.; Cheeseman, J. R.; Zakrzewski, V. G.; Montgomery, J. A., Jr.; Stratmann, R. E.; Burant, J. C.; Dapprich, S.; Millam, J. M.; Daniels, A. D.; Kudin, K. N.; Strain, M. C.; Farkas, O.; Tomasi, J.; Barone, V.; Cossi, M.; Cammi, R.; Mennucci, B.; Pomelli, C.; Adamo, C.; Clifford, S.; Ochterski, J.; Petersson, G. A.; Ayala, P. Y.; Cui, Q.; Morokuma, K.; Malick, D. K.; Rabuck, A. D.; Raghavachari, K.; Foresman, J. B.; Cioslowski, J.; Ortiz, J. V.; Stefanov, B. B.; Liu, G.; Liashenko, A.; Piskorz, P.; Komaromi, I.; Gomperts, R.; Martin, R. L.; Fox, D. J.; Keith, T.; Al-Laham, M. A.; Peng, C. Y.; Nanayakkara, A.; Gonzalez, C.; Challacombe, M.; Gill, P. M. W.; Johnson, B. G.; Chen, W.; Wong, M. W.; Andres, J. L.; Head-Gordon, M.; Replogle, E. S.; Pople, J. A. *Gaussian 98*, revision A.7; Gaussian, Inc.: Pittsburgh, PA, 1998.
(13) Becke, A. D. *J. Chem. Phys.* **1993**, *98*, 5648.
(14) Head Gordon, M.; Pople, J. A.; Frisch, M. J. *Chem. Phys. Lett.* **1988**, *153*, 503.
(15) Frisch, M. J.; Head Gordon, M.; Pople, J. A. *Chem. Phys. Lett.* **1990**, *166*, 275.
(16) Frisch, M. J.; Head Gordon, M.; Pople, J. A. *Chem. Phys. Lett.* **1990**, *166*, 281.
(17) Head Gordon, M.; Head Gordon, T. *Chem. Phys. Lett.* **1994**, *220*, 1.
(18) Head Gordon, M. *Mol. Phys.* **1999**, *96*, 673.
(19) Ditchfield, R.; Hehre, W. J.; Pople, J. A. *J. Chem. Phys.* **1971**, *54*, 724.
(20) Hehre, W. J.; Ditchfield, R.; Pople, J. A. *J. Chem. Phys.* **1972**, *56*, 2257.
(21) Hariharan, P. C.; Pople, J. A. *Theor. Chim. Acta* **1973**, *28*, 213.
(22) Gordon, M. S. *Chem. Phys. Lett.* **1980**, *76*, 163.
(23) Hariharan, P. C.; Pople, J. A. *Mol. Phys.* **1974**, *27*, 209.
(24) Pople, J. A.; Head Gordon, M.; Raghavachari, K. *J. Chem. Phys.* **1987**, *87*, 5968.
(25) Ochterski, J. W.; Petersson, G. A.; Montgomery, J. A., Jr. *J. Chem. Phys.* **1996**, *104*, 2598.
(26) Curtiss, L. A.; Raghavachari, K.; Pople, J. A. *J. Chem. Phys.* **1993**, *98*, 1293.
(27) Mo, O.; Yanez, M.; Esseffar, M.; Herreros, M.; Notario, R.; Abboud, J. L. M. *J. Org. Chem.* **1997**, *62*, 3200.
(28) Bouchoux, G.; Gal, J. F.; Maria, P. C.; Szulejko, J. E.; McMahon, T. B.; Tortajada, J.; Luna, A.; Yanez, M.; Mo, O. *J. Phys. Chem. A* **1998**, *102*, 9183.
(29) Bouchoux, G.; Defaye, D.; McMahon, T.; Likholyot, A.; Mo, O.; Yanez, M. *Chem.-Eur. J.* **2002**, *8*, 2900.